

Rho Meson Diffraction off Au Nuclei

R. Debbe for the STAR Collaboration

Brookhaven National Laboratory Upton NY 11973, USA

E-mail: debbe@bnl.gov

Abstract. The STAR Ultra Peripheral Collisions program has collected a substantial sample of ρ mesons and for the first time at RHIC energies it has been able to extract the distribution of momentum transfer t from diffractive elastic scattering off the Au ion. The resulting diffraction pattern is consistent with coherent scattering off a nuclear object the size of the Au nuclei. Measurements of this nature can offer insights and guidance to the ongoing preparations for the new electron ion programs.

1. Introduction

Our perception of nuclei has evolved drastically since the early days of Rutherford's experiments which made them appear as almost point like and massive objects. Higher energy electron scattering refined that knowledge providing the spatial distribution of charge in nuclei. The actual extent of the strong force was investigated with beams of pions and protons but that program suffered from the difficulties in disentangling the interference between Coulomb and nuclear interactions. At that point nuclei were well described by an almost spherical distribution referred to as the Wood-Saxon distribution. With the access to much higher energies, electron scattering opened a whole new way to study nucleons as it made accessible the study of their composite partonic nature. In particular, the HERA program identified the surprising fact that up to 20% of the interactions had the target nucleon left intact. This fact can be understood as the result of these high energy interactions being able to resolve partons which carry even smaller fractions of the nucleon momentum and are subject to non-linear effects. The ideal probe to study the nuclear component of nuclei would be one that does not carry charge. Such a probe can be found in the photon fluctuations; a photon of enough energy can be itself or it may fluctuate into neutral vector mesons, quark pairs or lepton pairs with corresponding decreasing probability. Such beams of photons and its fluctuations are available at the RHIC and LHC colliders. High fluxes of photons described with the Weizsäcker-Williams formalism [1] are present at RHIC with energies that range up to 24 GeV in the photon-nucleon center of mass.

We report the measurement of the transverse momentum of the ρ^0 meson after it undergoes an elastic scattering on the corresponding Au ion. For the first time, a diffraction pattern with several secondary peaks is clearly visible. Previous similar measurements were performed at low energy at SLAC [2] and at DESY with bremsstrahlung photons [3], in both cases the distributions of transverse momentum of the ρ mesons only shows the main diffraction peak. This measurement comes as preparations are taking place for a new Electron Ion Collider (EIC) that will revolutionize, one more time, our ability to study nucleons and nuclei. This new program will, in addition to existing variables used to characterize the state of partons, include information about their distribution in the transverse plane. That information will be extracted

from distributions similar to the ones reported in this work as the transverse momentum of the recoil target is a conjugate of the impact parameter of the collision.

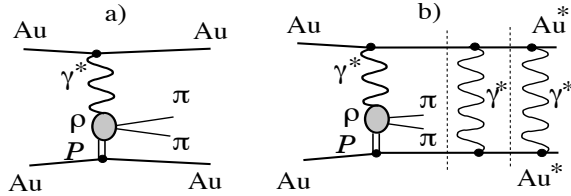


Figure 1. Schematic diagrams for UPC events. Panel a shows the most unbiased events. Panel b shows UPC events with further photon exchanges that excite both nuclei.

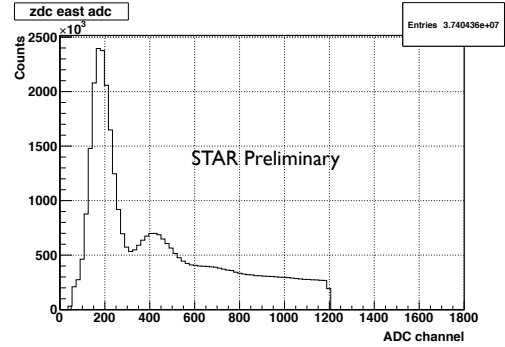


Figure 2. The distribution of charge collected in one of the ZDC detectors, a clear one neutron peak is visible followed by a smaller one related to two neutrons.

2. The STAR Experimental setup

The data used for this analysis were collected with the STAR detector at RHIC from Au+Au collisions with center of mass energy per nucleon $\sqrt{s_{NN}}=200$ GeV. The momentum of charged particles were detected with the STAR Time Projection Chamber (TPC) in two units of pseudo-rapidity centered around 0 ($|\eta| < 1$) and full azimuthal coverage. The TPC records up to 45 samples of the ionization left in the detector gas which allows for a good resolution particle identification based on energy loss. The charge left by particles inside the TPC drifts along its axis and is read out on the East and West sides which are divided into six sectors each. The TPC is also used to identify the vertex of the collisions and together with the bending power of the 0.5 Tesla magnetic field, it provides a momentum resolution equal to $\Delta p_T/p_T = 0.005 + 0.004p_T$. More details about the TPC can be found in [4]. The cylindrical TPC is completely surrounded by the Time Of Flight (TOF) detector consisting of 23040 Resistive Parallel Plate gas detectors arranged in cells, groups of which form modules installed in two sets of trays along the East and West sides of the TPC, 10 TOF trays overlap the azimuth coverage of one TPC readout sector. The TOF detector was used to trigger the UPC events and provides good time-of-flight measurements, although this analysis doesn't make use of that information. STAR has two Zero Degrees Calorimeters (ZDC) installed at ± 18 meters away from the nominal interaction point. These calorimeters are optimized for the detection of beam energy neutrons. These detector are instrumental in the definition of the trigger used for this analysis, more details about them can be found in [5].

2.1. Triggers

At the time the data used for the present analysis was collected, two triggers were defined to collect events described by the diagrams of Fig. 1. The event shown in panel a of that figure are collected with a trigger named UPC_Topo and events similar to those depicted in panel b were collected with the so called UPC_Main trigger. For both triggers the TOF detector is used to set limits in the number of tracks detected in the event. The ZDC calorimeters are used to identify events where the nuclei undergo a Coulomb excitation (a Giant Dipole Resonance GDR) decaying into one or more neutrons emitted along the beam. The Beam Beam Counter (BBC)

is used as a veto of events with any activity at high rapidity. The UPC_Topo trigger is the most inclusive of the triggers and is designed to tag the least biased UPC events; the ones without constraints on the number of neutrons detected in the ZDC calorimeters. This trigger is based on the TOF detector ability to find a pair of back-to-back particles by selecting events with TOF hits in two azimuthally opposite sectors (as mentioned above, a sector is formed with 10 trays). To avoid contamination from cosmic rays impinging vertically on the TPC the top (0) and bottom (3) sector are used as vetoes.

The cross section for ρ photoproduction tagged by UPC_Topo trigger is ~ 10 times higher than the one for the UPC_Main events [6], but the less restrictive nature of the first trigger makes it inefficient as it collect many spurious events, in contrast the UPC_Main trigger is cleaner and more efficient because of the conditions imposed on the number of neutrons detected in the ZDC detector.

2.2. Data sets

This report is based on the analysis of 22.9 million UPC_Main events written to tape by the STAR data acquisition system. This represents two thirds of the total number of events collected that year. (Events from an earlier part of that run period may be included in future analyses once further tests are conducted on the appropriate setup of the trigger.) Once the data is fully reconstructed a first selection of events is made. During run 10 the luminosity of RHIC was high enough such that the TPC being a slow detector had recorded several collisions (it takes $\sim 36 \mu$ sec for the ionization left by a track close to the middle of the detector to drift to the readout planes). The events that are read in this first pass can contain several vertices. The analysis of each events starts by looping over the vertices, pairs of tracks originating from the same vertex are formed whenever the vertex was constructed out of at most 12 tracks. These pairs are then written to root tree files. Each track in the pair carries all the information extracted from the TPC as well as the corresponding TOF relevant variables whenever available. Information about energy deposited in the EM calorimeter cells is also written for each track. The root tree files are then processed separately to identify the events that where identified ρ mesons were produced exclusively in events that recorded a single neutron in the ZDC calorimeters.

3. The ρ^0 meson identification

During the third and final pass on the data, events are first selected to have no more than one neutron in each one of the ZDCs, this selects the 1n1n exitation of the ions. Figure 2 shows the pedestal subtracted signal from the East ZDC, The cut for a single neutron is placed at ADC channel 300. Tracks that are part of the triggered events are identified through their vertex and the one associated to the TOF hits present in the data. Pairs that do not have that connection to the TOF hits that triggered the events are rejected. Figure 3 shows one event in the YZ view of the TPC, tracks originating from the same vertex are presented as lines of the same color. The tracks shown with black lines are the ones connected to at least one TOF hit.

The identity of each track in the selected pairs is obtained from the amount of ionization energy deposited along their trajectory inside the TPC volume. Tracks that have less than 14 samples (hits) are eliminated from the set because they are found to be produced by low momentum particles spiraling along the solenoidal magnetic field. The resolution of the dE/dx measurement in the TPC is very good and allows a clean identification of pions up to $\sim 1 GeV/c$ covering the range of momenta for pions originating from ρ mesons produced practically at rest. Figure 4 shows the correlation between dE/dx and the momentum of the particles. Pions are clearly visible as the mostly horizontal band of “minimum ionization”. With this identification it is now possible to select events that contain pion pairs. Pairs with different charge will then be considered as candidates decays from a ρ^0 meson. Pairs of tracks with equal charge $++$ or $--$ are also used to build our best estimate so far of the background for the production of ρ^0

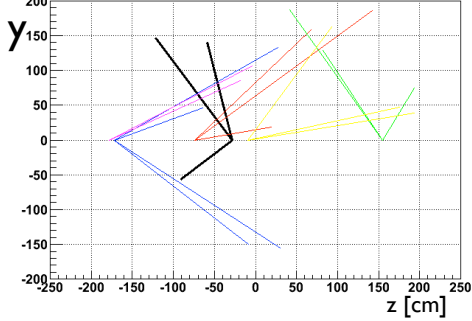


Figure 3. The projection of tracks on the YZ view of the STAR TPC is shown with black lines for a UPC triggered event. Other events recorded in the TPC are shown with different colors.

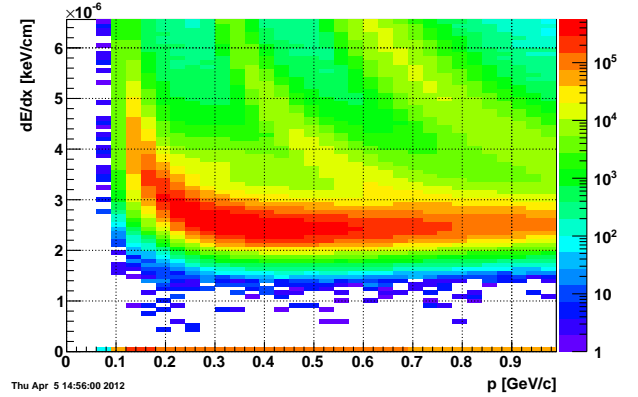


Figure 4. The average ionization energy loss (in keV/cm) recorded for tracks detected in the TPC is shown as function of their measured momentum (in GeV/c). The pion band is dominant in this figure but both kaon and proton bands are also visible.

mesons in UPC events. The invariant mass of both types of pairs is constructed and is shown in Fig. 5 where the black histogram shows the mass distribution for pairs of opposite charge, and the red one shows the mass distribution from equal charge pairs, which from now on will be considered as the background to this ρ^0 meson study. The wide mass distribution centered at 770 MeV is dominant in the black histogram, as well as a very narrow peak at the kaon mass, most likely produced by the decay of K_S^0 into two pions.

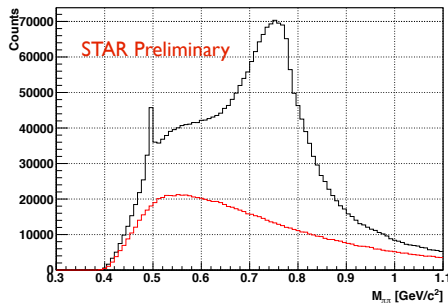


Figure 5. Invariant mass distribution for pion pairs of opposite charge shown with a black histograms, together with the similar distribution filled with pion pairs of equal charge.

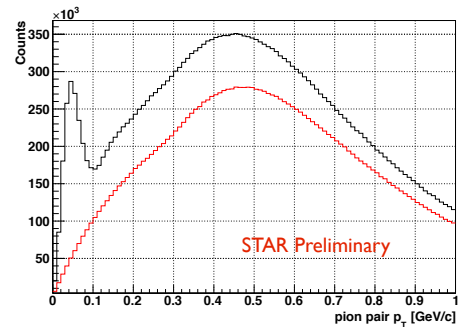


Figure 6. Transverse momentum distribution of pairs of opposite charge are shown with a black histogram. The red histogram shows similar distribution but this time for pion pairs of equal charge.

Figure 6 shows the distribution of the transverse momentum of the pion pair for opposite charge pions in the black histograms and the same charge pion pairs shown in the red histogram. The distribution shows a prominent peak below 100 MeV/c and a much broader distribution at higher value of p_T . The low transverse momentum peak is related to ρ mesons scattering

coherently off the Au ion. In other words, the uncertainty principle connects the narrow low p_T peak with a broad spatial structure; the Au nucleus. An earlier STAR publication [7] dealing with UPC ρ^0 meson coherent production imposed a cut on the p_T of the pion pair at 150 MeV/c to select coherent scattering, in this analysis no such cut is applied and a subtraction of the incoherent component of the ρ scattering is used to enhance the coherent events. The assumption made is that the coherent component has a rapidly falling tail that extends to higher values of p_T and is completely hidden in Fig. 6 by the less steeply falling incoherent component as well as by the increasing contribution of background contamination. The best estimate of the pion background in our data sample is the corresponding shape and magnitude of the equal sign pairs in every studied distribution, as done in the STAR publication [8].

The last condition applied to the pairs on this third pass requires that the vertex of the selected event is formed with only two tracks. This condition, together with the veto imposed on the BBC detectors should then make our sample of ρ^0 mesons as exclusively produced in UPC events.

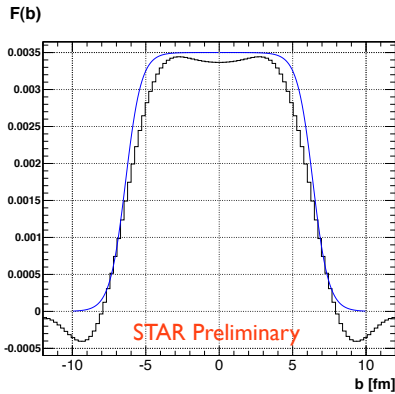


Figure 7. One dimensional Fourier transformation of the measured diffraction pattern shown as a black histogram. The Wood Saxon functional form with $R=6.38$ fm and $a_0 = 0.535$ fm is shown with a blue curve.

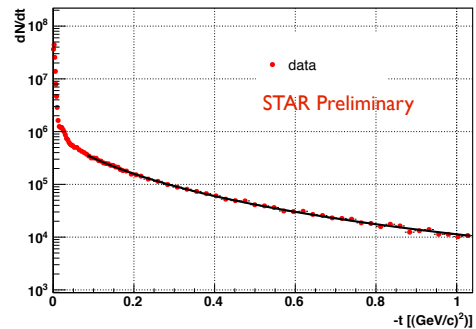


Figure 8. Background subtracted distribution of ρ mesons as function of $-t$ shown with red markers. A fit to a power law function is shown with a black curve. No acceptance correction is applied.

The ρ meson is finally defined with cuts applied to the invariant mass distribution of the pion pairs that satisfied the conditions listed above. The lowest value cut on mass is set at 500 MeV and the top value of the same cut at 1 GeV.

4. The diffraction pattern

We make the important assumption that the t of the ρ^0 meson completely balances the one of the target Au ion and what we are producing is the t distribution of the recoil ion. The appropriateness of such assumption will be discussed again when we compare the measurements to model calculations.

The t Mandelstam variable for the ρ defined as $t = (P_1 - P_3)^2$ where the four-vectors P_1 and P_3 are related to the ρ meson before and after the elastic interaction with the Au ion. In the lab. frame this quantity is written as $t = t_{min} - p_T^2$ where $t_{min} = -M_{\pi^+\pi^-}^2 / (2\gamma_L e^{|2y|})$ with γ_L being the Lorentz boost of the ion beam (equal to 108 at top RHIC ion energy) and y the rapidity of the ρ mesons. The value of t_{min} is small and was included for completeness.

Two histograms with variable bin size are prepared to be filled with the value of t for the exclusively produced ρ mesons detected in events with GDR excitations in both Au ions recording a single neutron in each ZDC. The bin width ranges from $0.0015 (GeV/c)^2$ at $t \sim 0$ to $0.024 (GeV/c)^2$ at $t = 0.3(GeV/c)^2$. The bin size was chosen to be always wider than the corresponding t resolution ($\Delta t/t = 0.01 + 0.008\sqrt{t}$). One histogram ($dN_{\rho}^{candidates}/dt$) is used to record the $-t$ distribution of opposite sign pions pairs. The other histogram ($dN_{background}/dt$) is filled with the value of $-t$ for pion pairs of equal charge. As mentioned above, this second histogram is considered to carry all the information about the background to ρ photo-production in UPC events. Studies to characterize the validity of this choice are still under way. At every bin, the contents of both histograms are divided by the corresponding bin width to produce the actual distributions. The $dN_{background}/dt$ distribution is then subtracted bin by bin from $dN_{\rho}^{candidates}/dt$ and the statistical errors are recalculated. The resulting distribution (dN_{ρ}^{signal}/dt) is shown with red dots in Fig. 8 where the first diffractive peak is clearly visible at $-t \sim 0$, a clear hint of the second diffractive peak is also present at this point in the analysis. A long slowly falling tail is present at higher values of $-t$. At this point the assumption is made that the coherent component of the ρ meson scattering off the Au nuclei is negligible and the totality of this tail is populated by incoherent interactions with individual nucleon. A fit to a “power law” shape ($A/(1 + |t|/p_0)^n$) is performed for $-t > 0.2 (GeV/c)^2$. This functional form reproduces well the incoherent tail ($\chi/NDF = 0.97$, $A = 7.609 \times 10^4$, $p_0 = 0.23 \pm 0.1$ and $n = 2.8 \pm 0.4$). The separation between coherent and incoherent contributions to the elastic scattering of the ρ meson on the Au nuclei is done statistically by subtracting the value of the fitted function at each bin center of the background subtracted distribution (dN_{ρ}^{signal}/dt). The resulting distribution is shown in Fig. 9 where all normalization and other corrections were applied.

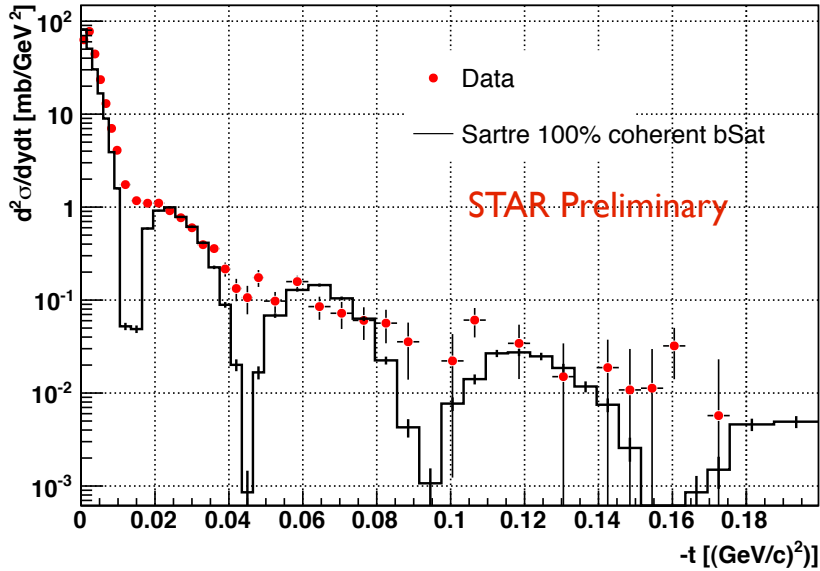


Figure 9. The diffraction pattern extracted from elastic scattering from the Au nuclei shown with red markers. The black histogram is the result of a calculation performed with Sartre.

The ρ meson reconstruction efficiency and the magnitude of the TPC acceptance are extracted making use of of STAR embedding procedures; pion pairs from the decay of one million ρ^0

mesons generated in UPC events with the StarLight [6] event generator are simulated and their trajectories and energy deposited along them are produced with a complete and up to date GEANT simulation of the STAR detector setup as it was at the time of RHIC run 10. The hits recorded in this simulation are then merged with information recorded during actual data taking in run 10 with the most unbiased trigger (zerobias). Embedding into these events produces the best description of the background in UPC events; a mix of pile-up, beam gas events as well as low multiplicity hadronic interactions. The complete STAR reconstruction chain is then used to process these data and the result is presented in several formats. To extract a first version of the reconstruction efficiency and the acceptance, a summary output was used where the information about the input generated particles as well as the parameters of the reconstructed tracks that match to a generated particle. The matching between reconstructed tracks and generated particles is based on the number of common hits. Ratios between 2D histograms counting matched and generated particles were calculated for different combinations of the ρ meson variables: transverse momentum and rapidity, azimuthal angle and rapidity and $-t$ and rapidity. The value of efficiencies \times acceptance as function of $-t$ was extracted. For the study reported here the rapidity dependence is averaged and the resulting value of the correction is equal to 44% and is found to be flat in $-t$.

The integrated luminosity for the runs included in this analysis is equal to $679(\mu b)^{-1}$ and is based on one of the STAR minimum bias triggers (*minbias_monitor*) which is estimated to cover up to 6 barns of the total Au+Au cross section.

4.1. Comparison to model calculations

The histogram shown in Fig. 9 was produced with the Sartre event generator [9] which in turn is based on the impact parameter dependent saturation model bSat [10]. Ten million ρ mesons were generated with the model set to mimic the Au+Au Ultraperipheral collisions at RHIC. The geometry of the target Au ion is simulated in a Glauber based Monte Carlo with individual nucleons distributed according to a Wood Saxon distribution with $R=6.38$ fm and $a_0 = 0.535$ fm. The cross section of the quark dipole is connected to the gluon distribution in the target nuclei and in particular, the black histogram in Fig. 9 includes the effects of saturation. The agreement between the data and the simulation is remarkable. The slopes of both first peaks are close to each other, the location and magnitude of the other diffraction peaks formed in the measurement are also well reproduced by the calculation. To first order, this agreement is strong indication that the methods used to isolate the coherent component of the ρ elastic scattering in the present analysis were correct, even though a quantification of such agreement remains to be done. A change in the di-quark cross section in the Sartre event generator which this time does not include the effects of saturation produces strong changes in the position of the deeps in the calculated diffraction pattern as is shown with the magenta histogram in Fig. 10

The Fourier transform of the measured diffraction pattern has been calculated making use of the azimuthal symmetry of the system : $f(b) = \int_0^{2\sqrt{t_{max}}} \sqrt{F(x^2)} J_0(xb/\hbar c) \frac{x}{2\pi} dx$ The result of the transformation is shown as a histogram in Fig. 7, together with the outline of the Wood-Saxon distribution drawn with a blue curve. No attempt has been made yet at assigning a systematic uncertainty to this calculation. The high b sides of the transform are related to $-t \sim 0$ in the diffraction pattern and the fact that they take negative values may be an artifact of bin size or the presence of destructive interference already measured in the same system [11]. The region close to $b=0$ is not well defined because the measurement has poor statistics at high $-t$. The falling edges of the distribution will turn out to be the best suited to extract some physics out of this measurement. Figure 11 shows the comparison between the diffraction pattern extracted from data (red markers) and the one calculated with the Starlight event generator (blue markers). This comparison shows a remarkable agreement on the depths of the diffraction deeps which

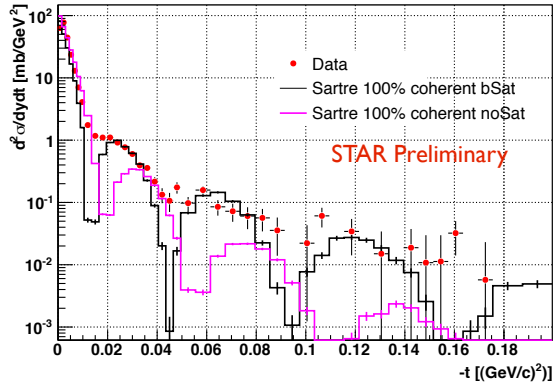


Figure 10. Diffraction pattern shown with two Sartre calculations, one with the presence of saturation in the gluon distribution of the ion target shown as a black histogram, and the other where such non linear effect have been turned off, is shown with a magenta histogram.

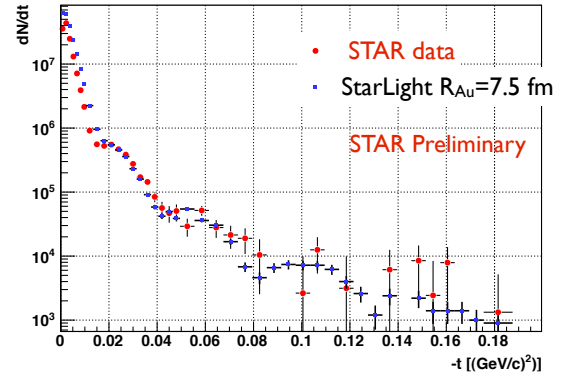


Figure 11. The unnormalized distribution for the $-t$ value of ρ mesons generated with Starlight is shown with blue markers to compare them with the same distribution extracted from data. The comparison highlights the good match of peaks and valleys in both cases.

within the Starlight calculation are the result of non zero transverse momentum component in the Weizsäcker-Williams photon exchanged between the ions [12]. A similar calculation performed for UPC events at 130 GeV produced shallow diffraction dips [13]. Such facts make our original assumption of purely longitudinal photons too simplistic but it does not preclude the possible unfolding of the photons transverse momentum contribution from our present results.

5. Summary

The STAR UPC program has measured coherent elastic scattering off Au nuclei with beams of exclusively produced ρ^0 mesons in Ultra Peripheral Collisions of Au ions at $\sqrt{s_{NN}} = 200$ GeV. The diffraction pattern extracted using the p_T of the scattered meson may not be an exact match to the one measured with the recoiling target ion, but such goal appears attainable with the help of a QED calculation to unfold the transverse contribution from the Weizsäcker-Williams photons. This measurement opens up a possible program to study the gluon form factor of nuclei, albeit with a restricted reach in Q^2 .

References

- [1] Bertulani C *et al.* 2005 *Ann. Rev. Nucl. Part. Phys.* **55** 271
- [2] Bulos F *et al.* 1969 *Phys. Rev. Lett.* **22** 490
- [3] Alvensleben H *et al.* 1970 *Phys. Rev. Lett.* **24** 786
- [4] Anderson M *et al.* 2003 *Nuclear Instrum. Methods* **A499** 659
- [5] Adler C, Strobele H, Denisov A, Garcia E, Murray M *et al.* 2001 *Nucl. Instrum. Meth.* **A461** 337–340
- [6] Baltz A Klein S and Nystrand J 2002 *Phys. Rev. Lett.* **89** 012301
- [7] Adler C *et al.* 2002 *Phys. Rev. Lett.* **89** 272302
- [8] Abelev B I *et al.* (STAR) 2008 *Phys. Rev.* **C77** 034910 (*Preprint* 0712.3320)
- [9] Toll T and Ulrich T 2011 vol INT-PUB-11-034 p 385 (*Preprint* nucl-th/1108.1713)
- [10] Kowalski H and Teaney D 2003 *Phys. Rev.* **D68** 114005 (*Preprint* hep-ph/0304189)
- [11] Abelev B *et al.* 2009 *Phys. Rev. Lett.* **102** 112301
- [12] Klein S and Nystrand J 2000 *Phys. Rev. Lett.* **84** 2330
- [13] Frankfurt L, Strikman M and Zhalov M 2003 *Phys. Rev.* **C67** 034901